

Properties and characterization of low-temperature amorphous PECVD silicon nitride films for solar cell passivation

S. ALI, M. GHARGHI, S. SIVOTHTHAMAN

*Department of Electrical and Computer Engineering, University of Waterloo,
200 University Avenue West, Waterloo, Ontario N2L 3G1, Canada*

K. ZEAITER

*Spherical Solar Power Inc., 250 Royal Oak Road, Cambridge, Ontario N3H 5M2, Canada
E-mail: sivoththaman@uwaterloo.ca*

Deposition conditions and some structural and electrical properties of amorphous silicon nitride ($\text{Si}_x\text{N}_y\text{:H}$) films deposited on Si substrates have been studied for photovoltaic applications. A plasma enhanced chemical vapor deposition (PECVD) system has been used for the study. Experiments have been performed varying the flow ratios and dilution of the reactant gases. Increased hydrogen (H_2) dilution leads to reduced deposition rate and a better controllability in the growth process. The hydrogen content in the film also decreases with increasing H_2 dilution of the reactant gases. Flow ratio of the reactant gases (SiH_4/NH_3) also influences the growth rate. There is an optimal reactant gas mix to maximize the film growth rate. However, the film stoichiometry is also modified by changing the gas mix, with higher flow ratios resulting in Si-rich films. The level of interfacial recombination of minority carriers has been studied by capacitance-voltage and effective lifetime measurements. Bombardment by the energetic species in the plasma leads to plasma damage at the interface. These interfacial defects can be annealed by a post-deposition, low temperature treatment. © 2005 Springer Science + Business Media, Inc.

1. Introduction

Amorphous silicon nitride ($\text{Si}_x\text{N}_y\text{:H}$) deposited by plasma enhanced chemical vapor deposition (PECVD) has been a topic of intensive investigation in the past several years. Studied plasma deposition techniques include electron cyclotron resonance (ECR) plasma [1], remote [2] and RF [3] plasma, to name a few. Plasma nitrides have a wide range of applications such as gate dielectrics in thin film transistors, metal-insulator-semiconductor field effect transistors [4–6], as well as encapsulation layers for electronic devices. Moreover, $\text{Si}_x\text{N}_y\text{:H}$ films have also been found to be very useful in crystalline Si photovoltaic (PV) devices [see for example, 7–9]. In Si PV cells, the nitride films provide an efficient passivation by reducing the surface recombination velocity at the Si/ Si_xN_y interface. It is also possible to achieve hydrogen passivation of Si bulk defects by the nitride process. This is especially important when low cost Si materials such as multicrystalline Si, Si ribbons etc., are used as substrates. In addition to these advantages, $\text{Si}_x\text{N}_y\text{:H}$ films also act as anti-reflection coatings on the solar cell surface. The structure and stoichiometry of low temperature deposited amorphous $\text{Si}_x\text{N}_y\text{:H}$ films are complicated and are strongly influenced by deposition conditions such as, the type of plasma excitation, temperature, pressure, gases and flow rates. In addition, any plasma-induced damage at the Si/ Si_xN_y

interface is also very critical in the surface passivation of Si PV cells. Techniques such as hot wire CVD [10] and remote plasma CVD [7] result in minimal or no surface damage. In this work we perform various sets of experiments in a PECVD nitride deposition system in order to gain a comprehensive understanding of the effect of processing conditions on the film and interfacial properties. Structural and electrical properties of the nitride films as well as the influence of post-deposition thermal treatments on any eventual plasma-induced damage at the interface are investigated.

2. Experimental

2.1. Film deposition and sample preparation

The hydrogenated $\text{Si}_x\text{N}_y\text{:H}$ films were deposited on *p*-type Si wafers in a conventional parallel plate 13.56 MHz PECVD deposition system. The wafers were always cleaned using the standard RCA solutions and HF-dipped prior to being loaded in the system. We used SiH_4 and NH_3 as precursor gases and H_2 as a dilutant. The ratio between SiH_4 and NH_3 gas flows, as well as the degree of H_2 dilution was varied for various experiments. The depositions were carried out at 300°C with the RF power kept at 25 W. Table I summarizes the experimental matrix. For the Fourier Transform

TABLE I Flow ratios of the reactant gases and the degree of hydrogen dilution used for the deposition of the $\text{Si}_x\text{N}_y\text{:H}$ films

Sample #	Flow ratio of SiH_4/NH_3 (sccm/sccm)	Hydrogen dilution (sccm)
N1	5/50	0
N2	5/50	30
N3	5/50	60
N4	5/50	90
N5	10/50	0
N6	10/50	30
N7	10/50	60
N8	10/50	90
N9	10/20	0
N10	10/20	30
N11	10/20	60
N12	10/20	90

Infrared Spectroscopy (FTIR) analysis, the Si wafers were deposited with relatively thicker ($1 \mu\text{m}$) nitride films. For the analysis of interface trap density (D_{it}) $\text{Al}/\text{Si}_x\text{N}_y\text{:H}/\text{Si}/\text{Al}$ capacitors were fabricated by sputtering Al on nitride-coated Si samples followed by patterning into arrays of capacitor structures ($36756 \mu\text{m}^2$) using photolithography. The nitride film thickness in each case was measured by a surface profilometer on patterned steps on the film. For the effective minority carrier lifetime (τ_{eff}) measurements by RF Photoconductivity Decay (RF-PCD) method, Si samples were coated with nitride on both sides under identical conditions. The lifetime samples underwent post-deposition anneals in a clean furnace at various temperatures in the range of $350\text{--}475^\circ\text{C}$ in N_2 ambient.

2.2. FTIR measurements

FTIR measurements were carried out in the 400 to 4000 cm^{-1} range, for the $\text{Si}_x\text{N}_y\text{:H}$ films deposited with different SiH_4/NH_3 ratios and H_2 dilutions. A baseline correction was performed. Peaks corresponding to Si–H and N–H bonds were identified from the absorption spectra and the relative densities of the bonds were determined, from which the H-content was calculated using standard technique.

2.3. Capacitance-voltage (C-V) measurements

High frequency (1 MHz) C-V characteristics of the fabricated $\text{Al}/\text{Si}_x\text{N}_y\text{:H}/\text{Si}/\text{Al}$ capacitor structures were measured using a Keithley Model 590 CV system. The sample was kept in the dark and 5 measurements were taken in different places for each sample. The C-V curves were then used to calculate the interface trap density (D_{it}) at the $\text{Si}_x\text{N}_y\text{:H}/\text{Si}$ interface.

2.4. Effective minority carrier lifetime measurements

Radio-frequency Photoconductivity Decay (RF-PCD) measurements were performed to determine the effective minority carrier lifetime (τ_{eff}) of the sample coated on both sides with $\text{Si}_x\text{N}_y\text{:H}$ films. The measurement

system uses a 532 nm laser pulse for excitation. The decay of the photoconductivity with time is recorded, from which τ_{eff} is extracted from the slope of the linear portion of the decay profile [11]. For each wafer, 5 measurements were taken at different places and the values were averaged.

2.5. Post-deposition thermal annealing

The lifetime samples were annealed in a clean, open-tube, quartz furnace in N_2 ambient at different temperatures in the range of $350\text{--}475^\circ\text{C}$. The effective lifetime was measured again on these samples in order to investigate the annealing of plasma-induced defects at the $\text{Si}_x\text{N}_y\text{:H}/\text{Si}$ interface.

3. Results and discussion

3.1. Film deposition rate

Fig. 1 shows the deposition rate of $\text{Si}_x\text{N}_y\text{:H}$ films as a function of H_2 dilution in the plasma chamber for various SiH_4/NH_3 gas ratios. Within the set of parameters used in our experiments, the general trend that we observe is that the growth rate decreases with increasing hydrogen dilution, irrespective of the SiH_4/NH_3 ratio. With increasing hydrogen dilution the partial pressures of the reactive gases are reduced. Therefore the availability of the reactants is diminished, leading to a reduction in deposition rate. The reduction in partial pressure can also help eliminate/reduce gas phase reactions which usually produce larger molecules that lead to poor quality films. With increased hydrogen dilution, the plasma-generated hydrogen atoms can cause saturation of hydrogen-lacking radicals, especially those of NH_3 . This will also reduce the deposition rate. The data in Fig. 1 shows that one can achieve a good control on growth rate by hydrogen dilution even when other parameters such as RF power and temperature are kept constant. Another important observation from Fig. 1 is that the dependence of the deposition rate on the SiH_4/NH_3 flow ratio. The data consistently show that, for any given H_2 dilution, the deposition rate passes through a “maximum”: the deposition

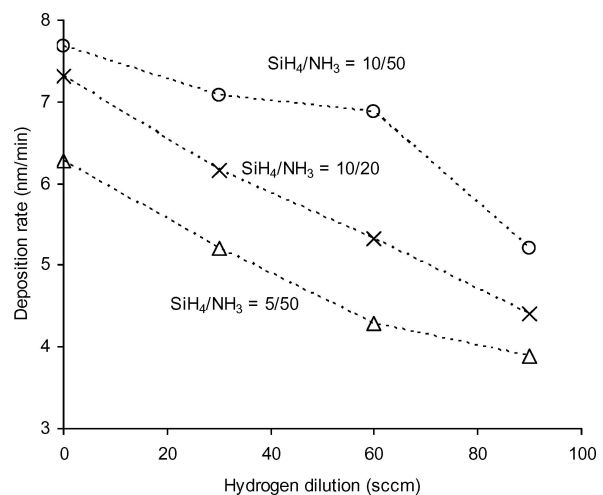


Figure 1 Deposition rate of $\text{Si}_x\text{N}_y\text{:H}$ films as a function of hydrogen dilution of reactant gases for various flow ratios of the reactant gases.

rates corresponding to a flow ratio of 0.2 (= 10/50) is always higher than those corresponding to flow ratios of 0.5 (=10/20) and 0.1 (=5/50). This suggests there is a balanced gas phase Si and N density that will lead to the highest deposition rate. On the other hand, it is important to note that varying the SiH_4/NH_3 flow ratio will vary the stoichiometry of the deposited film resulting in very different electrical and structural properties.

3.2. Film composition

Fig. 2 shows the absorption bands corresponding to Si-H stretching vibrations (2160 cm^{-1}) for $\text{Si}_x\text{N}_y\text{:H}$ films deposited with 3 different SiH_4/NH_3 flow ratio and with zero H_2 dilution. Among the 3 flow ratios that we have used, the highest flow ratio (0.5) results in the largest Si-H peak. Similarly Fig. 3 shows the absorption bands due to N-H stretching vibrations

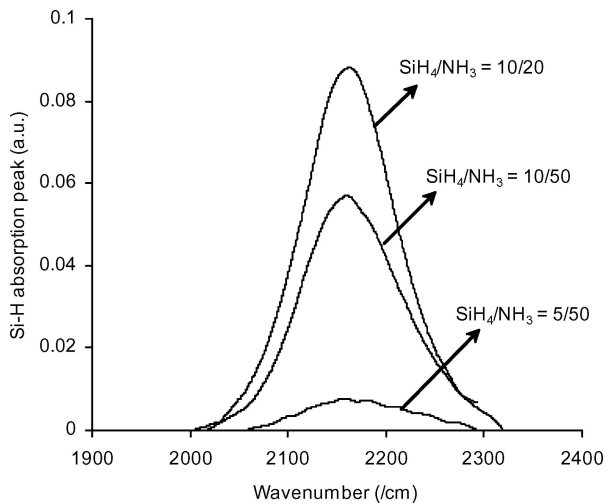


Figure 2 FTIR spectra of the absorption bands corresponding to Si-H stretching vibrations in the nitride films deposited using different gas flow ratios (without H_2 dilution).

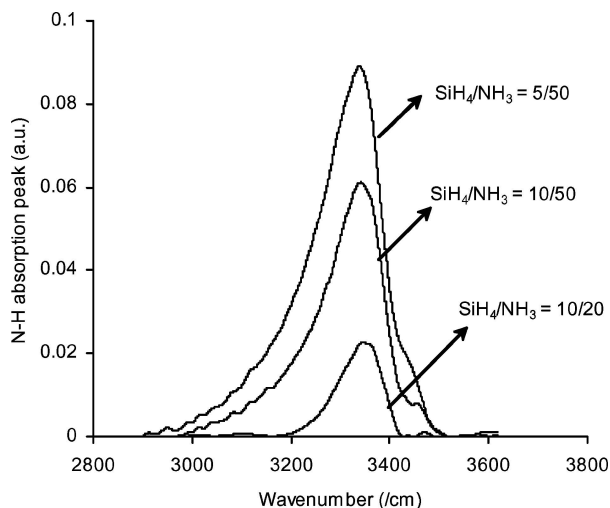


Figure 3 FTIR spectra of absorption bands corresponding to N-H stretching vibrations in the nitride films deposited using different gas flow ratios (without H_2 dilution).

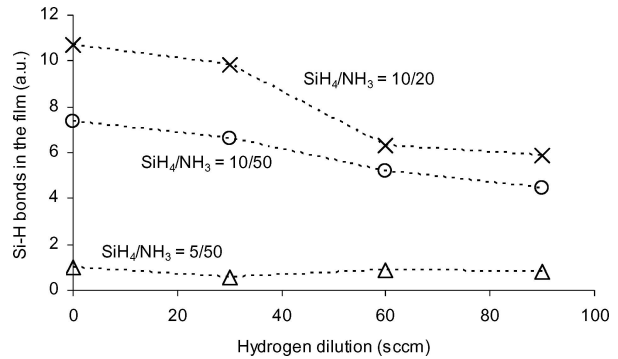


Figure 4 Intensity of Si-H bonds as extracted from the FTIR spectra for all the samples different H_2 dilutions and reactant gas flow ratios.

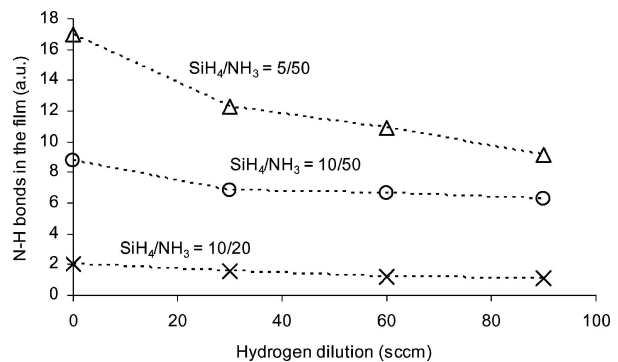


Figure 5 Intensity of N-H bonds as extracted from the FTIR spectra for all the samples different H_2 dilutions and reactant gas flow ratios.

(3350 cm^{-1}), for zero H_2 dilution, where the trend is just the opposite: the highest flow ratio (0.5) results in smallest N-H peak. This is somewhat expected: as the SiH_4/NH_3 flow ratio is increased (0.1 to 0.5) the films are expected to have a high Si content. The same trend was observed for other levels of H_2 dilution as well. Figs. 4 and 5 show the complete data (all flow ratios and H_2 dilutions) for the Si-H and N-H absorbance peaks respectively. With increasing H_2 dilution the dependence of N-H and Si-H intensities on the flow ratio seems to be slightly decreasing. Further, with increasing H_2 dilution, the strongest peaks (i.e., Si-H for a flow ratio of 0.5, and N-H for a flow ratio of 0.1) drop more significantly compared to the peaks of other flow ratios. Fig. 6 shows the H-content in the films for all the cases considered. The H-content has been deduced from the FTIR spectra [12]. The general trend is that the H content in the film decreases with increasing H_2 dilution. This can be attributed to the mechanism in which H atoms saturate the species lacking single hydrogen. Such species, when adsorbed to the surface, can add to the H-content in the film. By removal of those species, radicals with fewer H atoms take part more in the surface reactions, resulting in films with lower H-content. A closer look at Fig. 6 reveals that the decrease of H-content in Si-rich samples (mainly stemming from Si-H bonds) is not as steep as that in N-rich samples (mainly stemming from N-H bonds) as H_2 dilution is increased. This implies that hydrogen interacts with species originating from NH_3 more substantially than SiH_4 radicals.

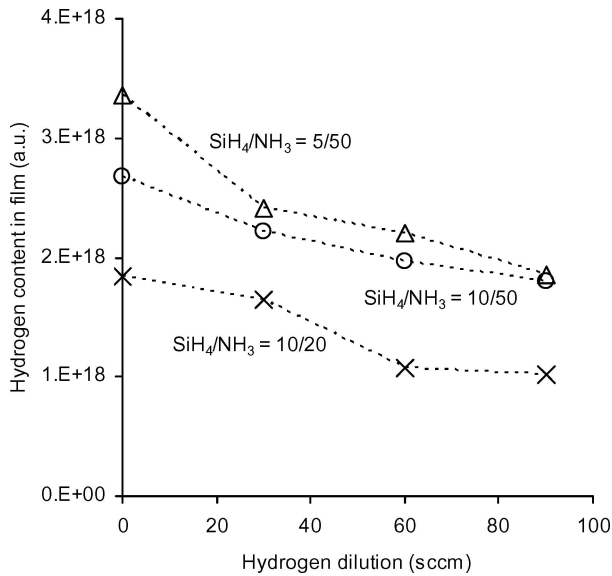


Figure 6 Hydrogen content in the nitride films deposited with different H₂ dilution of the reactant gases and reactant gas flow ratios.

3.3. C-V measurements: Interface trap density

The density of the interface traps (D_{it}) has been estimated from the measured high frequency C-V curves using the Terman method [13]. In this method the measured data is compared to an ideal theoretical curve and the D_{it} is extracted as a function of position in the Si bandgap. Fig. 7 shows a typical D_{it} curve obtained for the Si_xN_y:H/Si interface where the film was deposited with a SiH₄/NH₃ flow ratio of 0.1 (5/50) and without H₂ dilution. The D_{it} at the midgap (0.56 eV) is found to be around $9.93 \times 10^{11} \text{ cm}^{-2} \text{ eV}^{-1}$. These values indicate that the interface quality can still be improved. Table II gives the mid-gap D_{it} values obtained on several of our capacitors. The values are in the 10^{11} – 10^{12} range, and are rather scattered. Since we use a PECVD system for the film deposition, the interface has been exposed to bombardment by energetic species. Therefore there is a high possibility that there has been significant plasma-induced damage at the interface, and that this negative effect has been dominant in all the samples. Note that the RF power (25 W), pressure (150 mTorr) and deposition time (25 min) were kept constant for all our capacitor samples. We have verified the interface

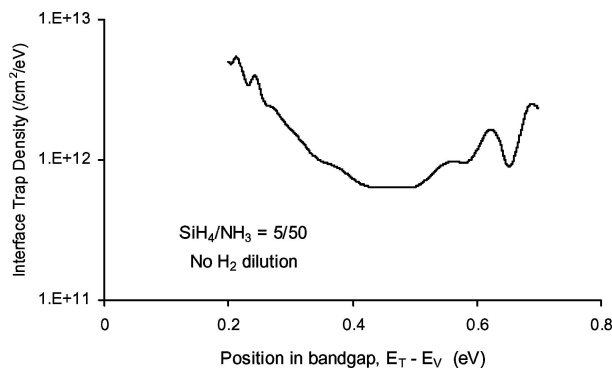


Figure 7 A typical interface trap density profile as extracted from high frequency C-V measurements on one of the Si_xN_y:H/Si capacitors. (nitride deposition condition: SiH₄/NH₃ = 5/50, without H₂ dilution).

TABLE II Interface trap density (D_{it}) of different samples extracted from high frequency capacitance-voltage (C-V) measurements

SiH ₄ /NH ₃ flow rate (sccm/sccm)	H ₂ dilution (sccm)	Interface trap density at midgap (cm ⁻² eV ⁻¹)
5/50	0	9.93×10^{11}
5/50	30	9.19×10^{11}
5/50	60	2.71×10^{12}
5/50	90	3.5×10^{12}
10/50	0	9.56×10^{11}
10/50	30	3.08×10^{12}
10/50	60	1.46×10^{12}
10/50	90	2.80×10^{12}

damage effect by subjecting some of the samples to post-deposition defect anneals. This is explained in the next section.

3.4. Effective minority carrier lifetime and post-deposition defect anneal

The effective lifetime (τ_{eff}) of the minority carriers was measured on wafers coated on both sides with Si_xN_y:H films. Fig. 8 shows the photoconductivity decay curve for the sample with films on both sides deposited with a 5/50 gas flow ratio and 30 sccm H₂ dilution. The τ_{eff} value extracted from the decay curve contains both the bulk and surface recombination components with the relationship, $1/\tau_{eff} = 1/\tau_b + 2S/d$, where “ τ_b ” is the bulk lifetime, “ S ” the surface recombination velocity, and “ d ” is the sample thickness. Therefore any changes in τ_{eff} after processes carried out at low temperatures can indicate a change in the surface passivation level provided the bulk lifetime is not affected. The values of τ_{eff} obtained for our samples were quite scattered irrespective of the film deposition conditions. This, as has been discussed in the previous section, again indicates the possibility of plasma damage causing interfacial recombination. To further investigate this, we

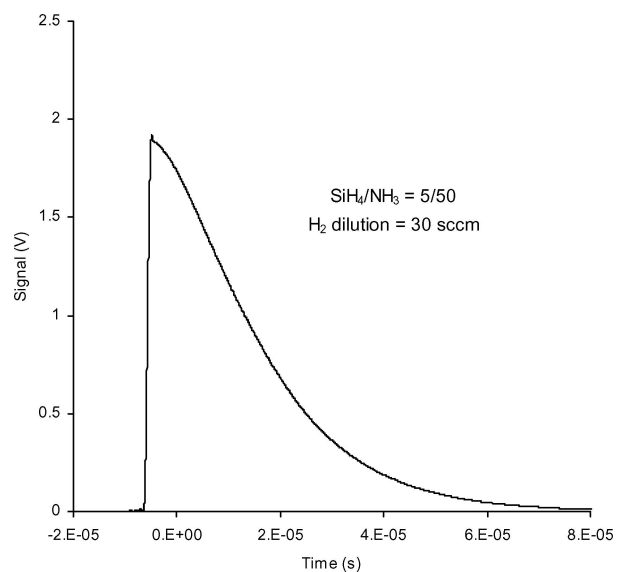


Figure 8 A typical photoconductivity decay profile of a nitride-coated Si sample. (nitride deposition condition: SiH₄/NH₃ = 5/50, H₂ dilution = 30 sccm).

TABLE III Measured effective lifetime (τ_{eff}) of nitride coated Si samples after being subjected to different temperature treatments. (conditions used for nitride deposition: SiH_4/NH_3 flow ratio = 5/50, H_2 dilution = 30 sccm)

Post-deposition annealing condition	Effective lifetime, τ_{eff} (μs)
as-deposited (no anneal)	14.45
350°C, 30 min	26.53
400°C, 30 min	21.55
425°C, 30 min	14.07
475°C, 30 min	10.63

TABLE IV Effective lifetime (τ_{eff}) of as-deposited and annealed samples. (annealing condition has been 350°C, 30 min for all samples)

SiH_4/NH_3 flow ratio (sccm/sccm)	H_2 dilution (sccm)	Effective lifetime:	
		as-deposited (μs)	after 350°C/30 min anneal (μs)
5/50	0	16.53	45.2
5/50	30	14.45	26.53
5/50	60	8.74	13.9
5/50	90	13.07	19.52
10/50	0	14.23	23.56
10/50	30	8.19	27.59
10/50	60	11.57	25.97
10/50	90	13.23	26.51
10/20	0	9.07	32.08
10/20	30	8.69	20.73
10/20	60	7.47	10.73
10/20	90	11.3	17.99

have subjected pieces of the sample to different thermal annealing treatments and measured the lifetime again. For example, the τ_{eff} corresponding to the decay in Fig. 8 is 14.45 μs . Table III shows the τ_{eff} of different pieces of the same sample after being subjected to different thermal anneals. Lower temperatures (<400°C) cause an improvement in τ_{eff} , indicating defect annealing. Higher temperatures however, seem to be causing the lifetime to drop again, most probably due to hydrogen loss from the interface leading to a poor passivation. This is quite possible because the annealing time was long (30 min). Table IV gives the τ_{eff} values of as-deposited and thermally annealed (350°C, 30 min) samples for different film deposition conditions. The lifetime improvement after the 350°C anneal is consistent in all the samples. In Table IV, the τ_{eff} of one sample cannot be compared to that of another sample because the bulk lifetime (τ_b) may be different. How-

ever, the improvement in surface passivation after the defect anneal is evident in all samples.

4. Conclusions

We have used a plasma PECVD system to study the properties of amorphous $\text{Si}_x\text{N}_y\text{:H}$ films. Several experiments have been performed varying the flow ratios of the reactant gases and hydrogen dilution. Increased hydrogen dilution leads to reduced deposition rate and a better controllability in the growth process. The hydrogen content in the film also reduces with increasing H_2 dilution of the reactant gases. Flow ratio of the reactant gases (SiH_4/NH_3) also changes the growth rate. There seems to be an optimal reactant gas mix to maximize the growth rate. However, the film stoichiometry is modified by changing the flow ratio. Higher flow ratios result in Si-rich films. The level of interfacial recombination of minority carriers has been studied by D_{it} analysis through C-V measurements, and by effective lifetime measurements. Bombardment by the energetic species in the plasma leads to plasma damage at the interface. The interfacial defects can be annealed by a post-deposition, low temperature treatment.

References

1. L. WANG, H. REEHAL, F. MARTINEZ, E. SAN ANDRES and A. DEL PRADO, *Semicond. Sci. Techn.* **18** (2003) 633, and references therein.
2. G. NOWLING, S. BABAYAN, V. JANKOVIC and R. HICKS, *Plasma Sci. Techn.* **11** (2002) 97.
3. G. NALLAPATI and P. AJMERA, *J. Vac. Sci. Techn.* **16** (1998) 1077.
4. M. POWELL, B. EASTON and O. HILL, *Appl. Phys. Lett.* **38** (1981) 794.
5. N. LUSTIG and J. KANICKI, *J. Appl. Phys.* **65** (1989) 3951.
6. A. SAZONOV, A. NATHAN and D. STRIAKHILEV, *J. Non-Cryst. Solids.* **266-269** (2000) 1329.
7. T. LAUINGER, J. SCHMIDT, A. ABERLE and R. HEZEL, *Appl. Phys. Lett.* **68** (1996) 1232.
8. L. CAI, A. ROHATGI, S. HAN, G. MAY and M. ZOU, *J. Appl. Phys.* **83** (1998) 5885.
9. S. BOWDEN, F. DUERINCKX, J. SZLUFCHIK and J. NIJS, *Optoelect. Rev.* **8** (2000) 307.
10. J. MOSCHNER, J. SCHMIDT and R. HEZEL, in Proc. 29th IEEE Photovoltaic Specialists Conference, New Orleans (IEEE Press, 2002).
11. R. AHRENKIEL, D. LEVI and J. ARCH, *Solar Energy Mater. Solar Cells* **41/42** (1996) 171.
12. W. LANFORD and M. RAND, *J. Appl. Phys.* **49** (1978) 2473.
13. E. NICOLLIAN and J. BREWS, "MOS Physics and Technology" (John Wiley, 1982).